Analytical and Bioanalytical Chemistry (2019) 411:2981–2993
https://doi.org/10.1007/s00216-019-01736-y

RESEARCH PAPER

Detection of very long-chain hydrocarbons by laser mass spectrometry reveals novel species-, sex-, and age-dependent differences in the cuticular profiles of three *Nasonia* species

Tanja Bien[1,2] · Jürgen Gadau[3] · Andreas Schnapp[1] · Joanne Y. Yew[4] · Christian Sievert[3] · Klaus Dreisewerd[1,2]

Received: 15 January 2019 / Revised: 22 February 2019 / Accepted: 1 March 2019 / Published online: 8 April 2019

Abstract

Long-chain cuticular hydrocarbons (CHC) are key components of chemical communication in many insects. The parasitoid jewel wasps from the genus *Nasonia* use their CHC profile as sex pheromone and for species recognition. The standard analytical tool to analyze CHC is gas chromatography coupled with mass spectrometric detection (GC/MS). This method reliably identifies short- to long-chain alkanes and alkenes, but CHC with more than 40 carbon atoms are usually not detected. Here, we applied two laser mass spectrometry (MS) techniques, namely direct laser desorption/ionization (d)LDI and silver-assisted (Ag-)LDI MS, respectively, to analyze CHC profiles of *N. vitripennis*, *N. giraulti*, and *N. longicornis* directly from the cuticle or extracts. Furthermore, we applied direct analysis in real-time (DART) MS as another orthogonal technique for extracts. The three methods corroborated previous results based on GC/MS, i.e., the production of CHC with carbon numbers between C25 and C40. However, we discovered a novel series of long-chain CHC ranging from C41 to C51/C52. Additionally, several previously unreported singly and doubly unsaturated alkenes in the C31-C39 range were found. Use of principal component analysis (PCA) revealed that the composition of the newly discovered CHC varies significantly between species, sex, and age of the animals. Our study adds to the growing literature on the presence of very long-chain CHC in insects and hints at putative roles in insect communication.

Keywords Laser mass spectrometry · *Nasonia* · Long-chain cuticular hydrocarbons · Principal component analysis · DART

Introduction

The cuticular hydrocarbon (CHC) profile on the surface of an insect is a key component in chemical communication between and within species [1, 2]. While the main original function of CHC within the chitin layer is thought to be waterproofing [3] over evolutionary time, cuticular lipids have taken on a plethora of additional biological functions. In particular, many CHC serve as molecular cues (or signals) in the contexts of species, mate, and colony recognition (e.g., for signaling the mating status of individual animals [4, 5]). The gain of new functions led to an immense chemical diversification of the CHC profiles, with numerous insect species exploiting a complex stereochemical repertoire to produce highly specific semiochemicals. Along with the total chain length, structural variations include methyl-branching, degree of unsaturation, and specific position of the carbon-carbon double bonds and their *E/Z* stereochemistry [6]. In addition

Electronic supplementary material The online version of this article (https://doi.org/10.1007/s00216-019-01736-y) contains supplementary material, which is available to authorized users.

✉ Jürgen Gadau
gadauj@uni-muenster.de

✉ Klaus Dreisewerd
dreisew@uni-muenster.de

[1] Institute for Hygiene, University of Münster, Robert-Koch-Str. 41, 48149 Münster, Germany

[2] Interdisciplinary Center for Clinical Research (IZKF), University of Münster, Albert-Schweitzer-Campus 1, 48149 Münster, Germany

[3] Institute for Evolution and Biodiversity, University of Münster, Hüfferstr. 1, 48149 Münster, Germany

[4] Pacific Biosciences Research Center, University of Hawai'i at Mānoa, 1993 East-West Road, Honolulu, HI 96822, USA

to aliphatic CHC, many species of insects also use polar lipids as communication cues, e.g., free fatty acids (FFA, [7]), fatty acyl alcohols [8, 9], triacylglycerols (TAG, [10, 11]), and a variety of other oxygen-containing molecules [6, 8]. If a stereocenter exists, the chiral *S/R* configuration may also be exploited by some insects to fine-tune species-specific communication [12].

The primary analytical methods used to study insect CHC profiles are gas chromatography coupled with mass spectrometry (GC/MS) or flame ionization detection (GC-FID) (e.g., [4]). However, a significant blind spot of these methods is that they can only detect compounds that are sufficiently volatile and can be fractionated on a GC column. In addition, diagnostic ions and the intact molecular ion have to be produced with sufficient abundance to enable structural identification. Generally, these boundary conditions restrict the use of standard GC/MS with electron ionization (EI) sources to CHC that contain no more than about 40 carbon atoms.

For standards of *n*-alkanes, molecular ions with chain lengths up to C75 have been generated by the use of "cold-EI," a technique in which a supersonic beam reduces the internal energies of the molecules prior to the ionization step [13]. To our knowledge, within the context of chemical ecology applications, cold-EI GC/MS has so far not been applied for the detection of CHC with carbon numbers beyond those already accessible by standard GC/MS [14].

More recently, several ionization techniques other than GC/MS were used for the MS analysis of long-chain CHC of insects. Cvačka et al. applied matrix-assisted laser desorption ionization (MALDI) to profile the CHC composition of various insects (termites, ants, cockroaches, and flesh flies) [15]. The detection of very long-chain CHC, partially in excess of C70, as $[M + Li]^+$ ions was made possible by derivatizing a classical MALDI matrix (namely, 2,5-dihydroxybenzoic acid, DHB) with isotopically enriched ^{7}Li. The advantage of using ^{7}Li with about 97% purity was that, in this way, adduct formation with a virtually monoisotopic cation was achieved, and isotopic correction of ^{6}Li/^{7}Li overlaps was avoided. In contrast to GC/MS, only the total chemical composition of the CHC (number of carbon atoms and degree of unsaturation) is obtained by MALDI-MS. In a follow-up study, individual *Drosophila melanogaster* vinegar flies were coated with a thin film of the lithiated DHB matrix. The animals were scanned with a focused laser beam to obtain a coarse image of the distribution of cuticular lipids across the body surface [16]. In other follow-up work, the same groups also introduced lithium derivatives for further MALDI matrices and tested those also for CHC analysis [17]. A disadvantage of the MALDI approach is the higher background of matrix ion–derived signals.

Yew et al. used direct analysis in real-time (DART) MS to profile the cuticular lipids of individual male and female *D. melanogaster* flies after sampling compounds by gently rubbing the fly surface with a metal pin [18]. In DART, metastable helium atoms serve for penning ionization of atmospheric molecules, in particular water clusters. Upon collisions with neutral CHC molecules, analyte ionization is achieved by proton transfer [19]. Therefore, predominantly, $[M + H]^+$ ions are generated with this technique. DART enables the analysis of a wide range of olefins and oxygen-containing compounds. A certain limitation, which requires careful data evaluation, is the possible occurrence of H_2 abstraction and further fragmentation reactions (e.g., cleavage of methyl groups) within the ionization process [20]. A variation of helium-based DART MS is the use of negative-ion mode DART. Cody et al. demonstrated that under certain conditions, this method can enable detection of *n*-alkanes as O_2-adducts [21].

In another work by Yew and co-workers, direct laser desorption/ionization, a method similar to MALDI but not requiring a chemical matrix, was used in combination with a collisional cooling ion interface that was mounted on an orthogonal time-of-flight mass analyzer (oTOF-MS). Alkenes and a series of oxygen-containing long-chain hydrocarbons (e.g., the fatty acyl alcohol (*3R,11Z,19Z*)-3-acetoxy-11,19-octacosadien-1-ol) were generated from *D. melanogaster* [9, 22]. With dLDI-oTOF MS, CHC are generally detected as $[M + K]^+$ ions in a fragmentation-free manner and, to a lower extent, as $[M + Na]^+$ species. Due to the use of a focused laser beam, dLDI lends itself for the screening of single animals with coarse lateral resolution (e.g., to differentiate body parts; [10, 23]). Because the ionization step in dLDI MS depends on the formation of energetically labile complexes between the analyte molecules and the alkali metal ions, so far only the detection of alkenes with at least one carbon-carbon double bond has been reported.

In another variant of a laser MS technique, named surface-assisted laser desorption ionization (SALDI), cuticular lipids are made available to the MS analysis by the use of light absorbing substrates. In particular, colloidal nano-silver has been successfully used [24, 25], because this transition metal offers both a high absorptivity at the wavelengths of the standard MALDI lasers of 337, 349, and 355 nm and generally a high coordination energy for adduct formation with olefins. We showed recently that upon applying samples onto etched porous silver substrates for Ag-LDI oTOF MS, the detection of alkanes with carbon numbers between C20 and C42 from standards and from extracts of various insects (e.g., *Apis mellifera* and *Anyana bicyclus*) became possible [26]. Due to the natural distribution of the ^{107}Ag and ^{109}Ag isotopes, comprising abundances of 51.84% and 48.16%, respectively, $[M + Ag]^+$ doublets with almost equal signal heights are produced by the technique.

In the present study, we applied dLDI, Ag-LDI, and DART mass spectrometry to "re-analyze" the cuticular hydrocarbon profiles of three species of the parasitoid wasp genus *Nasonia* (Hymenoptera: Pteromalidae), namely *N. vitripennis*,

N. giraulti, and *N. longicornis*. *Nasonia* is an established model system for evolutionary biology and has been extensively studied over the last 20 years with regard to the composition, genetic basis, and function of their CHC profiles [27–33]. Numerous behavioral studies showed that long-chain CHC act as female sex pheromone and are also used by both sexes for species recognition [30–32, 34]. However, it is unclear which components or ratios of components at which concentrations are used for these functions and whether all chemical compounds used in this intraspecific communication system are already known [35]. In particular, polar lipids could serve as potential candidates for sex/species pheromones [33]. For example, the male sex pheromones (4*R*,5*R*)- and (4*R*,5*S*)-5-hydroxy-4-decanolide (HDL) of *Nasonia vitripennis* were described by Ruther et al. [36] and the genetic basis for its differences between *N. vitripennis* and the other three known *Nasonia* species (*N. giraulti*, *N. longicornis*, and *N. oneida*) was revealed by Niehuis et al. [37]. That study showed that the two chiral isomers (4*R*,5*R*, and 4*R*,5*S*) are generally expressed in three out of four *Nasonia* species, whereas *N. vitripennis* expresses only one of the isomers (4*R*,5*S*). Two fatty acids, namely linoleic acid (LA) and oleic acid (OA) have been identified as precursors for HDL biosynthesis [38]. Notably, *Nasonia* belongs to the small group of animals that are able to convert OA into LA [38].

High molecular weight (MW) components of CHC profiles have recently been described for a range of other insects but it was not known whether the *Nasonia* spp. CHC profile also contains those components. The largest CHC component reported for *Nasonia* spp. so far, based on GC/MS, was C40 and, at trace abundances, C41 [27, 34]. The emphasis of our present study was to first corroborate and secondly expand the known CHC profiles of different *Nasonia* species. In particular, we searched for high molecular weight or polar components of the CHC profile that could have been missed due to the limitation of GC-MS. A second goal was to determine the CHC profiles for different developmental stages and sexes. For that purpose, we applied the three MS methods (dLDI, Ag-LDI, and DART MS) to individual virgin and mated males and females from *N. vitripennis*, *N. giraulti*, and *N. longicornis* directly after hatching and once they were 48 h old. Principal component analysis (PCA) of the CHC profiles was used to identify CHC components that contributed to the observed species, sex, age, and mating status-related differences in the cuticular CHC profiles.

Material and methods

Chemicals and materials

Heptane (chromatography grade) was from Merck (Darmstadt, Germany), 0.5-mm-thick silver foils (art. no. 98059959, purity > 99.9%) were from Jeddeloh (Winsen, Germany), pentane (≥ 95%), acetone (HPLC-grade), ethanol (≥ 99.5%), and HNO_3 (65%) were from Carl Roth (Karlsruhe, Germany), and the *n*-alkane standard mixture (C21-C40, 40 mg/L, each, dissolved in toluol, art. no. 04071) was from Fluka Sigma-Aldrich (Taufkirchen, Germany).

Rearing of insects

Highly inbred standard lines from all three *Nasonia* species, *N. vitripennis* (ASYMC), *N. giraulti* (RV2X), and *N. longicornis* (IV7X), were kept in climate chambers at 25 °C under constant 16/8-h light/dark cycles. Males and females were separated as 11–14-day-old pupae and were then kept in a separate vial until they emerged. To keep age relatively constant, we gave females only 1 h to sting a host (*Calliphora* spp.) and to lay eggs. The animal cohorts used in the MS experiments are summarized in Table 1. Collection time points of 0 (+ 1 h) and 48 h (± 1 h) after hatching were used for each sex. To initiate mating, two 48-h-old virgin male and female wasps were placed in a vial and observed until copulation took place. After copulation, the wasps were separated and handled as described below.

Biological and technical replicates

All Ag-LDI spectra were generated from an extract of an individual animal; pooled samples were used only for DART analysis. As detailed in Table 1, between 7 and 13 animals (depending on availability) were used for each of the 18 experimental groups. For virgin insects, we had 12 experimental groups (3 species × 2 sexes × 2 ages = 12) and for mated insects, we had 6 experimental groups (3 species × 2 sexes × 1 age/48 h). Three technical replicates were analyzed for Ag-LDI, while only one spectrum was collected for DART. For dLDI-MS, data were recorded in a qualitative manner, only, with the number of technical replicates ranging up to ten, depending on availability; for a few groups of sex and age, no animals were available for dLDI or the samples did not produce useful dLDI MS results.

Table 1 *Nasonia* cohorts used for the Ag-LDI MS measurements and subsequent PCA

Species/age		0 h/ virgin	48 h/ virgin	48 h/ mated
N. vitripennis	♀	10	11	9
	♂	11	9	10
N. longicornis	♀	11	10	11
	♂	13	13	10
N. giraulti	♀	12	10	10
	♂	7	12	10

Sample preparation for dLDI-MS

Animals were anesthetized with CO_2, killed by freezing, and stored in closed vials at − 80 °C until further use. Storage time was kept below 4 weeks. To avoid extensive condensation of moisture after removing the animals from the freezer, it was important to keep the vials closed until the samples fully warmed to room temperature. Preparation of whole animals on the MS sample holder was performed as described previously [23]. Briefly, adhesive pads (G304, Plano, Wetzlar, Germany) were used to mount individual animals on thin cover slips with 0.15-mm thickness. The glass slips were mounted in a custom-made sample holder with a rectangular, 1.8 mm deep well. Sample height was adjusted by choosing a stack of 0.2-mm-thick adhesive pads (G3347, Plano, Wetzlar, Germany). This step was important to achieve an optimal position, both relative to the laser beam and the ion extraction cone of the ion source.

Sample preparation for Ag-LDI MS

Preparation of etched silver substrates was carried out as described previously [26]. Briefly, the silver foils were first cut to about 4×4 mm^2 wide pieces. To remove surface contamination, the substrates were washed with a series of pentane, acetone, ethanol, and deionized water. Next, the foils were placed under a hydraulic press (~ 5 t/cm^2) to obtain thin, flat, substrates that were approximately 25–30 mm^2 wide. This was followed by a second washing step with deionized water, ethanol, acetone, pentane, acetone, and again ethanol and deionized water. Etching of the foils was achieved by placing them in 23% HNO_3 at 50 °C. The etching process was terminated after the surface obtained a grayish appearance; typically, this occurred within a few minutes. Our previous study [26] showed that the surface features achieved at this time exhibit mean dimensions in the low micrometer range. Etched silver plates were washed ten times with deionized water and stored in a container with pure deionized water before further use. Prior to the MS experiments, the substrates were allowed to dry before affixing them onto a standard stainless steel oMALDI-2 sample plate (AB Sciex, Concord, Canada) using 0.2-mm-thick adhesive pads (Plano). Care was taken that the silver substrates fully covered the surface of the pads. Care was also taken to avoid any contact of the substrates with plastic material.

Individual insects were placed in 0.1-mL glass vials and were immersed by gentle mixing in 10 μL of heptane or, for additional MS experiments, a mixture of chloroform and methanol (1:1; *v*:*v*). After 20 min, the supernatant was removed with a pipette and transferred to a fresh vial. For each data point, an aliquot of 0.2 μL corresponding to about 1/50 to 1/40 of the total extracted per individual animal was carefully spotted onto the central area of the etched silver foils.

Laser mass spectrometry

The orthogonal extracting mass spectrometer was described in detail, previously [39]. Within the *m/z* range of interest (130–1150), a mass resolution of ~ 8000 (FWHM) and mass accuracy of about 30 ppm were obtained. Only the positive ion mode was used. The prototype instrument was equipped with a modified oMALDI-2 ion source (AB Sciex, Concord, Canada), which enabled operation with an adjustable buffer gas pressure via custom-made software and electronics [23]. Buffer gas pressures of 1.2 and 2.0 mbar of N_2 were used in the Ag-LDI and dUV-LDI MS experiments, respectively. The TOF extraction voltage was set to 10 kV and the pusher frequency of the ion extractor to 7.4 kHz. The single Q0 transfer quadrupole of the hybrid mass spectrometer was operated in the RF-only mode; the lower transmission cutoff was set to *m/z* 130. MS data were acquired and partially evaluated with TOFmulti software (vs. 1.5.9., Spicer and Ens, Univ. of Manitoba, Canada); further modifications to this software for automatic peak detection were made in house. oMALDI-2 Server software (vs. 2.2.1, AB Sciex, Concord, Canada) served to translate the sample plate with a precision of about 20 μm. For the dLDI experiments, manual steering of the sample plate was first used to find optimal desorption/ionization conditions. To compensate for possible chromatographic effects, which are potentially caused by a differential migration of lipids on the silver plates, concentric circles were scanned in all Ag-LDI measurements.

For the dUV-LDI measurements, the beam of an N_2 laser (MNL 100-LD; LTB Lasertechnik Berlin, Germany) with an emission wavelength of 337 nm and a pulse duration of 3 ns was coupled into an approximately 1.5-m-long UV-grade glass fiber with 200 μm core diameter. The end surface of the fiber was imaged 1:1 onto the samples using a telescope. In this way, irradiation with a close-to-flat-top beam profile was achieved [39], a factor that minimizes unwanted irradiation damage to the cuticle [9, 23]. Due to the angle of incidence of 30° relative to the ion beam axis, the focal laser spot exhibited elliptic dimensions of about 200×400 μm^2. The fluence (pulse energy per area) used throughout the experiments was about 500 J m^{-2}; the laser pulse repetition rate was set to 30 Hz, the maximum provided by the used N_2 laser. The laser spot on the cuticle was visible via the observation CCD camera and the induced fluorescence. MS data were acquired using 900 laser shots per spectrum, corresponding to a data acquisition time of 30 s. Owing to the small size of the animals, the laser was first scanned over the dorsal surface of mounted animals until "good" signal intensities were obtained, then the data acquisition was started and the laser was just irradiating this spot.

To analyze the C21-C40 *n*-alkane standard, a variant of dUV-LDI MS ("FALDI"), described in detail in references [23, 40], was used; 0.15 μL of the mixture was spotted on a

wing of a female *D. melanogaster* vinegar fly. MS analysis was achieved by sampling the wing surface with 900 laser shots.

For the Ag-LDI MS experiments, a Q-switched, frequency-tripled Nd:YAG laser (Flare PQ UV 1000-30, InnoLight, Hannover, Germany) was focused as a free beam into the oMALDI-2 ion source via a second optical port. This laser had a wavelength of 355 nm, a pulse duration of ~2 ns, and a fixed pulse repetition rate of 1 kHz. The focal spot size was approximately 50×60 μm^2 wide. The focal fluence was adjusted to about 1500 J m^{-2}. Due to the 1 kHz pulse repetition rate of the laser, the applied data acquisition time of 30 s corresponded to 30,000 laser shots per recorded mass spectrum.

DART mass spectrometry

Positive ion mode DART experiments were performed with an AccuTOF-DART mass spectrometer (JEOL USA, MA) at a resolving power of 6000 (FWHM). Helium was used as reactant gas. The gas heater was set to 300 °C and the glow discharge needle put at a potential of 3.5 kV. Electrode 1 was set to 150 V, and electrode 2 (grid) was set to 250 V. Scan time was about 1 s per data point spectrum, with an acquisition range of *m/z* 60 to 1000. Centroided spectra were exported as ASCII files for further processing with Mass Mountaineer software (RBC Software, Portsmouth, NH). Peak assignments were based on the criterion that experimental and calculated *m/z* values corresponded within 0.007 u.

Principal component analysis

To identify CHC compounds that create heterogeneity between the different *Nasonia* groups, we used PCA as a multivariate statistical method. PCA was performed using the MetaboAnalyst platform (http://www.metaboanalyst.ca). Only Ag-LDI-derived data was subjected to PCA. This was because of the, compared to the other two methods, highest reproducibility from animal to animal. Generally, the same trends on the biology were, however, recorded with all three methods. Signal intensities for the CHC compounds were extracted from each mass spectrum using the modified TOFmulti software of the prototype oTOF mass spectrometer and adaptation of a mass list containing monoisotopic Ag^{107}-adducts of alkane and alkenes with carbon numbers from C30 to C52. The selection was based on a set of initial test experiments. A signal-to-noise (S/N) ratio > 2 was used as cutoff criterion. It should be noted that with oTOF mass spectrometry, deviating criteria apply than if the CHC analysis would have been conducted with standard GC/MS. As illustrated in Fig. S1 (see Electronic Supplementary Material, ESM), in the oTOF mass spectra a regular chemical noise background is produced at each nominal mass. This can probably be attributed to C12 clusters, although the exact mechanisms are not fully understood. Hydrogen-rich long-chain CHC exhibit a mass increment that enable a clear separation from this background, even if nominally the S/N ratio may in some case be < 1, if the noise is defined by the regular background pattern.

A second selection criterion was that the signals were detected by both dLDI and Ag-LDI MS. Ag-LDI MS data were uploaded to the MetaboAnalyst platform as Excel sheets. Missing values in the mass list, in which, in some cases, no ion signal with S/N > 2 was detected at a given *m/z* point, were replaced by the half of the minimum positive value in the overall dataset (for that given *m/z* point); this was assumed to define the detection limit to first order. Signal intensities were normalized to the sum for each CHC. Importantly, this protocol generated data sets with comparable mean intensities for all data points, despite the variation in total ion counts between individuals. The latter is observable in particular between bigger female and smaller male *Nasonia*. To further improve the statistical analysis, the transformed variables were standardized (i.e., mean centered and divided by the standard deviation of each variable). With this operation, only the relative change of the variables affects the principal components. The compounds which contributed most significantly to the separation of the experimental groups in the scores plots were identified from the loadings plot and their respective boxplots were extracted. Tables listing the compounds contributing most to the separation were created by a ranking of their loadings. Selected tables are provided in the ESM.

Results and discussion

Detection of novel components in the Nasonia cuticle by the use of laser mass spectrometry

Use of dLDI MS A representative dLDI mass spectrum, recorded from the dorsal side of a virgin female *N. vitripennis* (48 h old), is displayed in Fig. 1a. A list of all major detected CHC signals is provided in Table 2. Unlike GC/MS, structural CHC isomers are not differentiated by the dLDI method; thus, only the total chemical compositions are noted. Previous GC/MS studies have shown that for different *Nasonia* cohorts, mostly the quantity and ratios between specific CHC components vary rather than qualitative differences (i.e., the presence/absence) are important [29, 31]. For this reason and because absolute quantitation is generally difficult with LDI MS, no further differentiation with regard to species, age, and sex has been made in Table 2, apart for a few cases for which specific CHC were only detected on male (m) or female (f) wasps.

Several previous GC/MS studies have shown that members of the genus *Nasonia* express a homologous series of long-chain alkanes with carbon numbers ranging from C25 to about

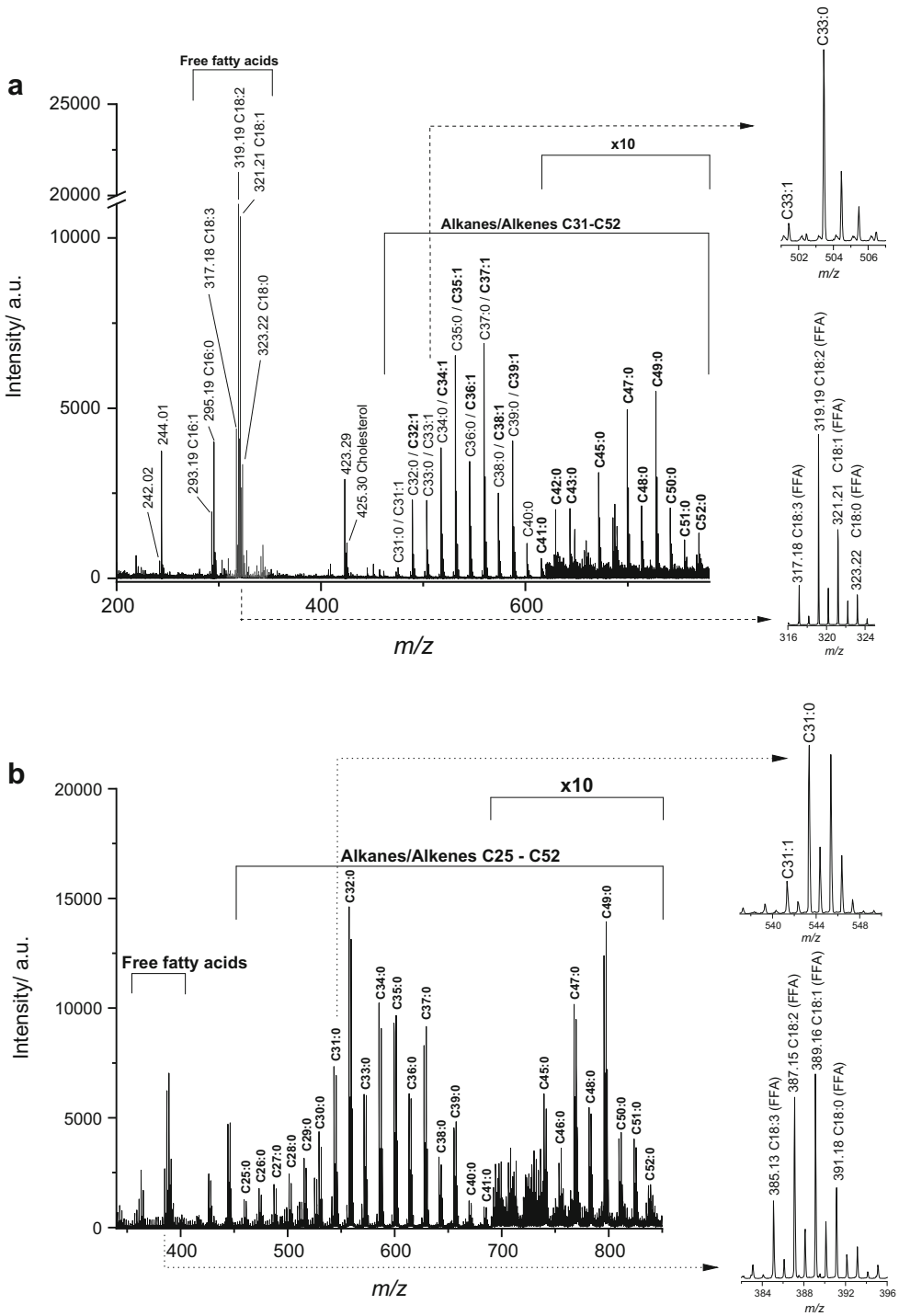

Fig. 1 **a** dUV-LDI mass spectrum acquired from the dorsal surface of a female *N. vitripennis* (virgin, 48 h old). Previously undescribed *Nasonia* lipids are highlighted in boldface. The insets show close-up views of the FFA C18:3-C18:0 and CHC C33:0/C33:1 signal groups, respectively. All ions represent $[M + K]^+$ adducts. An excerpt of a spectrum recorded from a male *N. vitripennis* is shown for comparison in Fig. S3 (see ESM). **b** Ag-LDI mass spectrum of heptane extract from a single female *N. vitripennis* (virgin, 48 h old). All lipids are in this case detected as $[M + {}^{107}Ag]^+$ / $[M + {}^{109}Ag]^+$ doublets

C40 [27, 29, 31, 34]. Above approximately C30, this series is reproduced by our dLDI MS data, whereas shorter chain CHC were generally not detected. An LDI MS experiment with an *n*-alkane standard (C21-C40), that was prepared on a *Drosophila* fly wing substrate according to the "FALDI" method of Yew et al. and Pirkl et al. [23, 40], indicated that the binding strength between the alkali metal ion and the hydrocarbon molecule is dependent on chain length. As such, only alkanes above about C30 are amenable to the dLDI-oTOF MS analysis (ESM Fig. S2). $[M + K]^+$ adducts of CHC with shorter chains are too labile to survive the desorption/ionization and mass analysis processes. Notably, the cutoff around C30 coincides approximately with the upper chain length of CHC as expressed by adult *Drosophila*, the insect system that has so far been most widely been analyzed by dLDI mass spectrometry [9, 10]. As a consequence, it was hitherto assumed that alkanes are not amenable to a dLDI MS analysis. Our new data show that this view has to be revised.

Table 2 List of CHC, FFA, and other compounds detected by dLDI, Ag-LDI, and DART MS; species that were not previously detected by GC/MS are highlighted in italics

Species	Chemical composition	$m/z(\text{dLDI})_{calcd}$/ $[M + K]^+$	$m/z(\text{Ag-LDI})_{calcd}$/ $[M + {}^{107}Ag]^+$	$m/z(\text{DART})_{exp}$/ $[M + H]^+$	dUV-LDI	Ag-LDI	DART	Reference (GC/MS)
Alkanes/alkenes								
C25:0	C25H52	391.37	459.31	353.41		+	+	[34]
C26:0	C26H54	405.39	473.33	367.43		+	+	[34]
C27:0	C27H56	419.40	487.34	381.45		+	+	[27, 34]
C28:0	C28H58	433.42	501.36	395.46		+	+	[27, 34]
C29:0	C29H60	447.43	515.37	409.48		+	+	[27, 29, 31, 34]
C30:0	C30H62	461.45	529.39	423.49		+	+	[27, 29, 31, 34]
C31:0	C31H64	475.46	543.41	437.51	o/~(f)	+	+	[27, 29, 31, 34]
C31:1	C31H62	473.45	541.39	435.49	+	+	+	[29, 31, 34]
C31:2	C31H60	471.43	539.37	433.48	+(m)	o	+	
C32:0	C32H66	489.48	557.42	451.52	+	+	+	[27, 29, 31, 34]
C32:1	C32H66	487.46	555.41	449.51	+	+	+	
C33:0	C33H68	503.50	571.44	465.54	+	+	+	[27, 29, 31, 34]
C33:1	C33H66	501.48	569.42	463.52	+	+	+	[29, 31, 34]
C33:2	C33H64	499.46	567.41	461.51	+	+	+	
C34:0	C34H70	517.51	585.45	479.56	+	+	+	[27, 29, 31, 34]
C34:1	C34H68	515.50	583.44	477.54	+	+	+	
C35:0	C35H72	531.53	599.47	493.57	+	+	+	[27, 29, 31, 34]
C35:1	C35H70	529.51	597.45	491.56	+	+	+	
C36:0	C36H74	545.54	613.48	507.59	+	+	+	[27, 29, 31, 34]
C36:1	C36H72	543.53	611.47	505.57	o	o	+	
C37:0	C37H76	559.56	627.50	521.60	+	+	+	[27, 29, 31, 34]
C37:1	C37H74	557.54	625.48	519.59	+	+	+	
C38:0	C38H78	573.57	641.52	535.62	+	+	+	[27, 29, 31, 34]
C38:1	C38H76	571.56	639.50	533.60	o	o	+	
C39:0	C39H80	587.59	655.53	549.63	+	+	+	[27, 29, 31, 34]
C39:1	C39H78	585.57	653.52	547.62	o	o	+	
C40:0	C40H82	601.61	669.55	563.65	+	+	+	[27, 29]
C41:0	C41H84	615.62	683.56	577.67	+	+	+	
C42:0	C42H86	629.64	697.58	591.68	o	o	+	
C43:0	C43H88	643.65	711.59	605.70	o	o	+	
C44:0	C44H90	657.67	725.61	619.71			+	
C45:0	C45H92	671.68	739.63	633.73	+	+	+	
C46:0	C46H94	685.70	753.64	647.74	o/*	o	+	
C47:0	C47H96	699.71	767.66	661.76	+	+	+	
C48:0	C48H98	713.73	781.67	675.77	+	+	+	
C49:0	C49H100	727.75	795.69	689.79	+	+	+	
C50:0	C50H102	741.76	809.70	703.81	+	+	+	
C51:0	C51H104	755.78	823.72	717.82	+	+	+	
C52:0	C52H106	769.79	837.73	731.84	~/o	~/o	~/o	
Free fatty acids								
C16:0	C16H32O2	295.20	363.15	257.25	+	+	+	[42, 43, 41]
C16:1	C16H30O2	293.19	361.13	255.23	+	+	+	[42, 43, 41]
C18:0	C18H36O2	323.20	391.18	285.28	+	+	+	[42]
C18:1	C18H34O2	321.22	389.16	283.26	+	+	+	[42, 43, 41]
C18:2	C18H32O2	319.20	387.15	281.25	+	+	+	[42, 43, 41]
C18:3	C18H30O2	317.19	385.13	279.23	+	+	+	[42]

Table 2 (continued)

Species	Chemical composition	m/z(dLDI)$_{calcd}$/ $[M + K]^+$	m/z(Ag-LDI)$_{calcd}$/ $[M + {}^{107}Ag]^+$	m/z(DART)$_{exp}$/ $[M + H]^+$	dUV-LDI	Ag-LDI	DART	Reference (GC/MS)
Other compounds								
HDL	C10H18O3	225.09	293.03	187.13	~/o(m)	–	+(m)	[37, 44]
Unknown	C27H44O	423.30	491.24	367.34 (-H_2O)	+	o/P	+	
Cholesterol	C27H46O	425.32	493.26	369.35 (-H_2O)	+	o/P	+	

+: consistently detected in most of the measurements

o: not consistently detected/at detection limit

~: detected only in some measurements

*: signal overlapped with those of near-isobaric ions

P: detected only in C/M extract

f: detected only in females

m: detected only in males

An improved collisional cooling of the generated gas phase ions or the use of a cool stage may in the future even allow to extend the MW limit to shorter CHC.

Different to the previous GC experiments, a second series of very long-chain alkanes with carbon numbers in excess of C40 is registered in the dLDI spectra. With high reproducibility, alkanes with carbon numbers up to C52 were found in all samples (Fig. 1a).

For both the long- (up to C40) and very long-chain series (>C40), odd-numbered CHC, in particular C37, C39, C47, and C49, generally produced the highest signals. This corroborates previous results of many GC/MS analyses of insect CHC profiles, albeit so far no generally accepted theory has been put forward to explain this bias.

We suspect that a lower expression level and some overlap with isobaric ions may have prevented the detection of the "missing" C44 and C46 peaks in the otherwise homologue CHC series.

Within the first long-chain CHC series (<C40), all singly unsaturated *Nasonia* alkenes as previously reported by GC/MS analysis (in particular the prominent C31:1 and C33:1 alkenes [27, 29, 31]) were reproduced by the dLDI experiments. In addition, within the C31 to C39 series, several new singly and doubly unsaturated alkenes are detected by dLDI (see Table 2 for a full list). In particular, C32:1 and C34:1 were recorded from male *Nasonia* cuticles with considerable intensities and some alkenes such as C31:2 were only detected in males (ESM Fig. S3a). These findings reflect the higher ionization efficiencies of dLDI MS for unsaturated and oxygen-containing HCs compared to fully saturated compounds [9, 23]. Unsaturated CHC with carbon numbers > 40 were not detected.

With our dLDI MS method, we could also confirm the presence of several polar lipids on the *Nasonia* cuticula. This includes a series of abundant FFA with compositions of 16:0 (palmitic acid), 16:1 (presumably sapienic acid), 18:0 (stearic acid), 18:1 (presumably oleic acid), 18:2 (presumably linoleic acid), and 18:3 (presumably linolenic acid), respectively (see inset in Fig. 1a). All of these FFA have been reported previously by GC/MS [42]; the imminent role of linoleic acid as a HDL precursor has been extensively discussed [38]. With dLDI MS, this male sex pheromone was discernible in some mass spectra with intensities close to the upper detection limit. This may be due to the irradiation of areas that are in close vicinity to the male sex pheromone producing glands (rectal papilla).

The intense ion at an m/z value of 425.29, that was recorded by dLDI MS from all *Nasonia*, regardless of age, sex, and species (Fig. 1a), likely corresponds to $[M + K]^+$ ions of cholesterol. Further experiments are needed to learn more about the chemical nature of the sister signal that was consistently observed at m/z 423.28. Because H_2 abstraction has so far generally not been found for dLDI MS, it may be speculated if this ion species may constitute a genuine compound (e.g., dehydrocholesterol).

Use of Ag-LDI MS Figure 1b shows a representative Ag-LDI mass spectrum that was recorded from a heptane extract of a virgin, 48-h-old female *N. vitripennis*. The spectrum corroborates the occurrence of the two CHC series as observed by dLDI mass spectrometry. A closer comparison of the dLDI and Ag-LDI data sets obtained from the same experimental groups, however, reveals some methodologically interesting differences. As was already demonstrated by Schnapp et al. [26], Ag-LDI MS is capable of detecting alkanes with chain lengths starting at C21. Consequently, all expected *Nasonia* alkanes with carbon numbers between C25 and C40, that were previously registered via GC/MS [27, 29, 31, 34], are found in the Ag-LDI mass spectra and, moreover, the very long-chain CHC series (C > 40) is also detected.

Due to the occurrence of the $[M + Ag]^+$ doublets and possible hydrogen abstraction reactions [26], a more careful data

evaluation is required compared with dLDI in order to differentiate between saturated and (poly-) unsaturated CHC by Ag-LDI MS. For example, this results in isotopic overlap of ^{109}Ag adducts from species with one or two double bonds with signals of their less unsaturated cognates. To a minor extent, the same holds for the natural occurrence of ^{41}K-isotopes (~ 7% abundance) for the dLDI data. Because the natural abundances of the metals are precisely known, it is however possible to deconvolute the spectra in a straightforward manner.

An experiment with a *n*-alkane standard showed that under our experimental conditions with carefully adjusted laser powers, the extent of these fragmentation processes falls into the < 10% range, compared to the intact molecular ion (ESM Fig. S3c). In comparison to dLDI MS, the silver-based method is also associated with a higher level of specific chemical background. For example, ions that were typically observed in all mass spectra at *m/z* values of 497.18 and 444.24, respectively, were recently identified as diisooctylphthalat and erucamid plasticizers [26].

Despite the above complications, when comparing dLDI and Ag-LDI mass spectra from male *N. vitripennis* (virgin, 48 h old, ESM Fig. S3a, b) with that from an *n*-alkane standard (ESM Fig. S3c), it is in most cases possible to qualitatively detect alkanes and singly to doubly unsaturated alkenes simultaneously with the Ag-LDI method even without application of signal deconvolution routines.

Use of DART MS The main findings of the laser-based measurements are also corroborated by DART MS, another sensitive, "orthogonal" ionization method. Analysis of extracts from the same animal groups as used for Ag-LDI (albeit in a pooled form) (Fig. 2) revealed the presence of the novel very long-chain CHC series up to C53, thus reproducing our findings with dLDI and Ag-LDI. Also, cholesterol is detected by DART MS.

When a mixture of chloroform/methanol was used as extraction solvents, CHC were generally detected with considerably lower signal intensities and predominantly, FFA and tri- and diacylglycerols as well as cholesterol are then observed by DART as well as Ag-LDI MS. In addition, several unknown compounds, which by accurate mass contain one or more oxygen atoms, are recorded from the more polar extract (data not shown).

Species-, sex-, and age-specific differences in the CHC profiles

In many species of insects, including *Nasonia*, CHC profiles as, e.g., probed by GC/MS, can be used for species, sex, and age differentiation [4, 45]. It is however much more difficult to know whether *Nasonia* itself uses the same cues to differentiate between these classes of individuals [29, 31, 35]. The surprising discovery of a novel series of long-chain alkanes for *Nasonia* in this study raises the question about the potential biological role of these compounds. One way to obtain a glimpse into functions of individual compounds of the CHC profile, although it is only correlative, is to test for consistent differences between different classes of individuals. Here, we used supervised principal component analysis (PCA) to separate species-, sex-, and age-dependent CHC profiles, with a focus on our newly discovered compounds. Due to its superior technical reproducibility, and the availability of multiple individual specific CHC profiles, the multivariate analysis was only performed with Ag-LDI data as obtained from all three investigated *Nasonia* species (*N. vitripennis*, *N. giraulti*, *N. longicornis*). Generally, the same clear trends (i.e., varying expression of CHC with, e.g., age or sex of the animal, for instance, higher intensities of odd-numbered chain length C35/C37/C39, C35/C47/C49) were however also observed by the use of dLDI MS. We analyzed the following groups: virgin males and females at ages of 0 h (eclosion) and 48 h, and furthermore also mated individuals at 48 h old to test whether mating itself changes CHC profiles. Molecular ion signals included in these analyses were comprised of all detected CHC with carbon numbers between C30 and C52.

Sex differences The scores plot that is obtained upon comparing the CHC components recorded for virgin male and female *N. vitripennis* (48 h old) is displayed in Fig. 3. At this age, individuals are mature and ready to mate. In the scores plot, males and females are well separated along the PC1 axis. The higher scatter of the data points for males along the PC2 axis might be attributed to the lower total amount of expressed CHC in these smaller individuals; note that, despite the different body sizes, constant volumes of extraction solvent and for the deposition onto the sample substrate were used for all samples. The loadings show that several of the newly detected CHC contribute significantly to the sex differences as revealed in the PCA analysis. Particular strong contributors (in the order of the impact of their loadings) are C34:0, C47:0, C49:0, and C39:0 for female, and several unsaturated CHC for male *N. vitripennis*, including C33:1 and C33:2. Box plots showing the normalized intensities for C33:1 and C34:0 are plotted at the right side of Fig. 3.

Similar results were found for male and female *N. giraulti* and *N. longicornis* at 48 h old (ESM Fig. S4). However, a few differences in terms of which compounds contributed most to the differentiation can be noted for the three *Nasonia* species. The four CHC components that contributed most strongly to the sex differentiation at 48 h for all three *Nasonia* species are summarized in Table S1 (see ESM). Compared to males of the same species, females generally express higher levels of the longer chain alkanes (e.g., C49). This effect is the strongest for *N. giraulti* and *N. vitripennis* and weaker for *N. longicornis*. In addition to C49, all females also express a significant amount of C39 and C47.

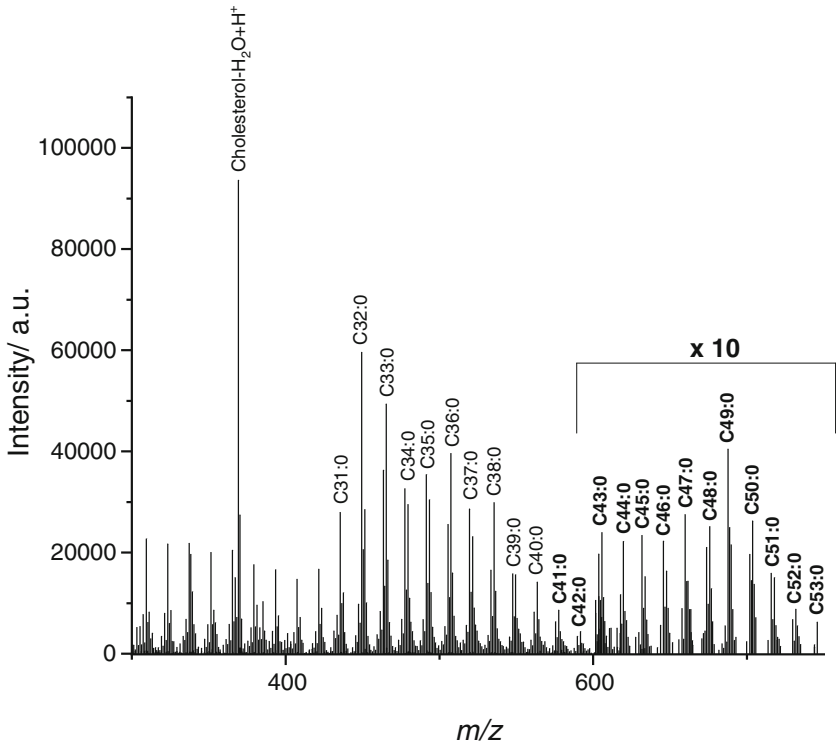

Fig. 2 Representative DART mass spectrum of a hexane extract from virgin female 48 h old *N. vitripennis*. Previously undescribed Nasonia lipids are highlighted in boldface. Taking H_2 and CH_3 abstraction into account, the same CHC patterns observed in dLDI and Ag-LDI experiments are obtained. In particular, a series of very long-chain CHC up to C53 is also detected with this orthogonal ionization technique

Development/age differences Compared to the 48-h-old animals, newly emerged male and female *Nasonia* spp. express almost similar CHC profiles (ESM Fig. S5). As individuals mature (within 24–48 h), the female CHC profile contains longer chain CHC and a lower percentage of alkenes, whereas male profiles retain a higher percentage of short-chain alkanes and more unsaturated compounds. These age-dependent modifications are not surprising and generally accompany, for example, maturation processes like ovarian development in social insects [46]. The four CHC components which contributed most strongly to the differentiation of 0- and 48-h-old *Nasonia* species are summarized in ESM Table S2 (scores plots not shown).

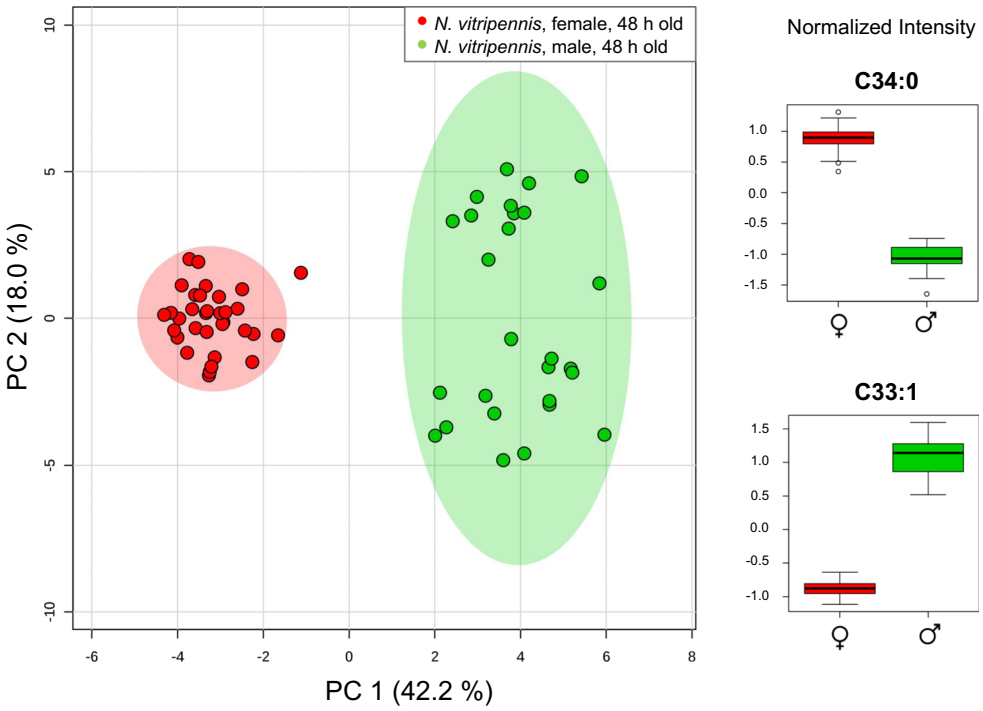

Fig. 3 Differentiation according to sex: Scores plot of 48-h-old male and female *N. vitripennis*. Box plots displaying the (normalized) intensity variation found for the two compounds that produced the highest loadings along PC1 are shown on the right. The four CHC components, which contributed most strongly to the sex differentiation at 48 h for all three *Nasonia* species are summarized in Table S1 (see ESM)

Species differences Females of all three *Nasonia* species are well separated into clusters in a 2D-PC1/PC2 scores plot (Fig. 4a). A dendrogram based on female CHC compound similarities (Euclidean Distance, Ward Clustering) reflects the correct phylogenetic relationships between the three species (ESM Fig. S6). In contrast, males are only separated if a three-dimensional scores plot including PC3 is applied (Fig. 4b). In an (evolutionary) biology context, these observations could be linked to the distinct role of CHC profiles as female sex pheromones, whereas no such function of CHC has so far been shown for males; rather, male *Nasonia* predominantly use a mix of more polar compounds; in the case of HDL, these are produced in rectal papilla [31, 36–38].

Effect of mating DART and dLDI MS analyses [9, 18] previously revealed that for *Drosophila*, CHC are exchanged between copulating individual. Temporarily, this results in

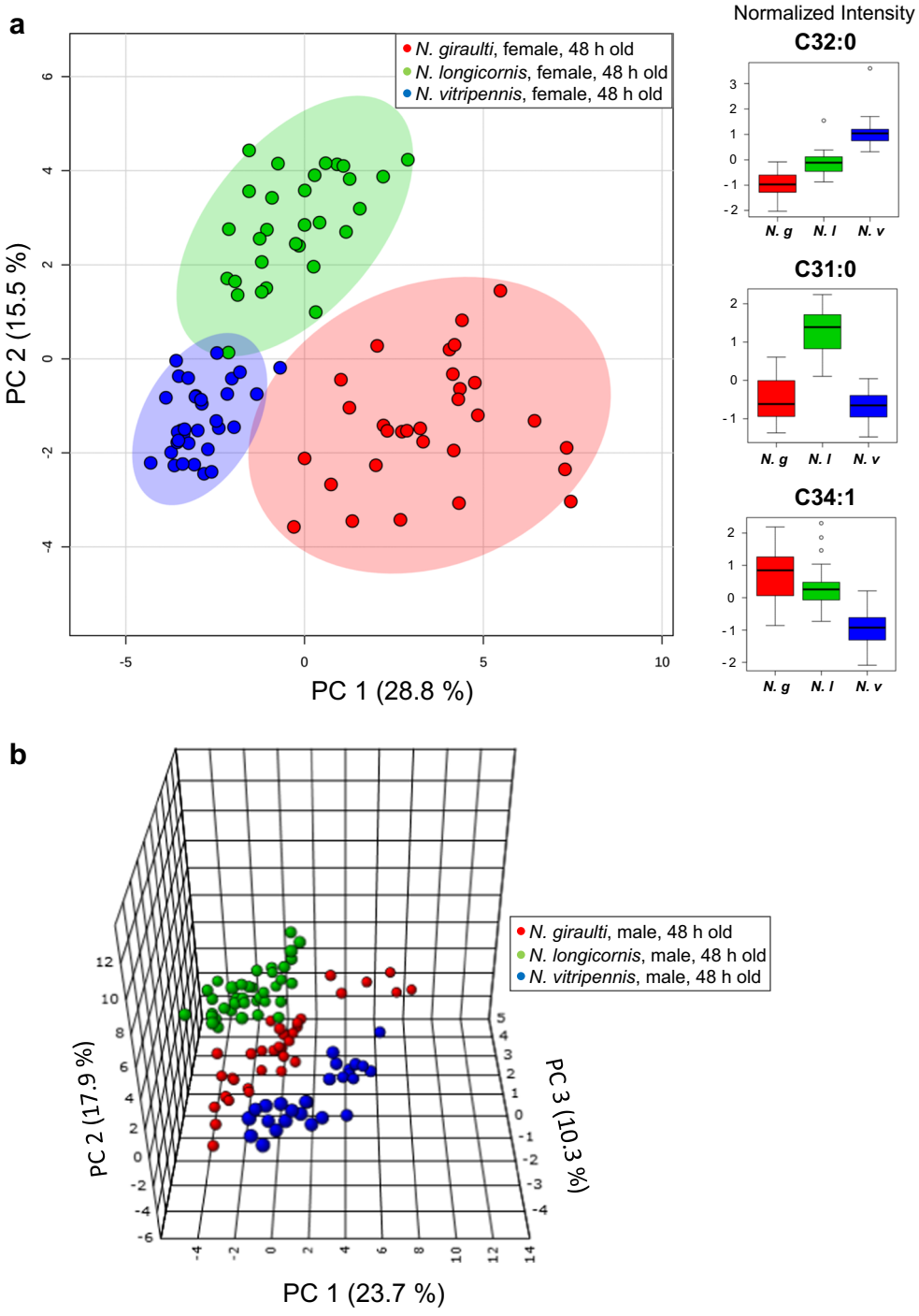

Fig. 4 Differentiation according to species for female and male *Nasonia*: **a** scores plot of virgin 48-h-old female *N. vitripennis*, *N. girault*, and *N. longicornis*. Box plots displaying the (normalized) intensity variation found for the three compounds producing the highest loadings along the separating PC are shown on the right. **b** 3D scores plot of 48-h-old male *N. vitripennis*, *N. girault*, and *N. longicornis*

significantly modified, mixed male/female cuticular profiles. A similar effect is also observed when the CHC profiles of recently mated 48-h-old male and female *Nasonia vitripennis* are compared (ESM Fig. S7). It is currently unknown whether these changes in CHC profiles have a direct consequence on behavior. Theoretically, the altered CHC composition could serve as a cue for males to identify mated from unmated females. This ability could increase male fitness since, for example, *N. vitripennis* females mate only once [30].

Conclusion

By the use of dLDI, Ag-LDI, and DART MS as discovery tools, several novel CHC species were recorded from the *Nasonia* cuticula that were previously not detected by standard GC/MS. In particular, very long-chain alkanes with carbon numbers in excess of C41 were registered for the first time. Our results add to the growing body of evidence that this class of hydrocarbons is found more frequently amongst insect class than previously thought. Statistical evaluation by PCA further revealed relative sex-, age-, and species-specific profile differences, a finding that suggests possible functions of these novel components as communication signals. Controlled behavioral studies will be needed to further look into these exciting possibilities.

Acknowledgements We thank Jens Soltwisch for the help with the oTOF mass spectrometer. Financial support by the German Research Foundation (DFG; grant DR 416/10-1 to K.D.), the Department of Defense US Army Research Laboratory (grant W911NF-16-1-0216 to J.Y.Y.), and the University of Münster for travel subsidies within their *Internationalisierungsstrategie* (to K.D.) is gratefully acknowledged.

Compliance with ethical standards

Conflict of interest The authors declare that they have no conflict of interest.

References

1. Lockey KH. Lipids of the insect cuticle: origin, composition and function. Comp Biochem Physiol B Biochem Mol Biol. 1998;89:595–645.
2. Howard RW. Cuticular hydrocarbons and chemical communication. In: Stanley-Samuelson DW, Nelson DR, editors. Insect lipids: chemistry, biochemistry and biology. Lincoln: University of Nebraska Press; 1993.
3. Gibbs AG. Water-proofing properties of cuticular lipids. Am Zool. 1998;38:471–82.
4. Blomquist GJ, Bagnères AG. Insect hydrocarbons: biology, biochemistry, and chemical ecology. Cambridge: Cambridge University Press; 2010.
5. Wyatt TD. Pheromones and animal behavior: chemical signals and signatures. 2nd ed. Cambridge: Cambridge University Press; 2014.
6. Yew JY, Chung H. Insect pheromones: an overview of function, form, and discovery. Prog Lipid Res. 2015;59:88–105.
7. Stanley-Samuelson DW, Jurenka RA, Cripps C, Blomquist GJ. Fatty acids in insects: composition, metabolism, and biological significance. Arch Insect Biochem Physiol. 1988;9:1–33.
8. Fröhlich B, Riederer M, Tautz J. Honeybees discriminate cuticular waxes based on esters and polar components. Apidologie. 2001;32:265–74.
9. Yew JY, Dreisewerd K, Luftmann H, Müthing J, Pohlentz G, Kravitz EA. A new male sex pheromone and novel cuticular cues for chemical communication in Drosophila. Curr Biol. 2009;19:1245–54.
10. Yew JY, Dreisewerd K, De Oliveira CC, Etges WJ. Male-specific transfer and fine scale spatial differences of newly identified cuticular hydrocarbons and triacylglycerides in a Drosophila species pair. PLoS One. 2011;6:e16898.
11. Chin JSR, Ellis SR, Pham HT, Blanksby SJ, Mori K, Koh QL, et al. Sex-specific triacylglycerides are widely conserved in Drosophila and mediate mating behavior. Elife. 2014;3:e01751.
12. Shikichi Y, Shankar S, Yew JY, Mori K. Synthesis and bioassay of the eight analogues of male pheromone CH503 (3-Acetoxy-11,19-octacosadien-1-ol) of the Drosophila melanogaster fruit fly. Biosci Biotechnol Biochem. 2013;77:1931–8.
13. Amirav A, Gordin A, Poliak M, Fialkov. Gas chromatography mass spectrometry with supersonic molecular beams. J Mass Spectrom 2008;43:141–163.
14. Lu B, Zelle KM, Seltzer R, Hefetz A, Ben-Shahar Y. Feminization of pheromone-sensing neurons affects mating decisions in Drosophila males. Biol Open. 2014;3:152–60.
15. Cvačka J, Jiroš P, Šobotník J, Hanus R, Svatoš A. Analysis of insect cuticular hydrocarbons using matrix-assisted laser desorption/ionization mass spectrometry. J Chem Ecol. 2006;32:409–34.
16. Kaftan F, Vrkoslav V, Kynast P, Kulkarni P, Böcker S, Cvačka J, et al. Mass spectrometry imaging of surface lipids on intact Drosophila melanogaster flies. J Mass Spectrom. 2014;49:223–32.
17. Horká P, Vrkoslav V, Hanus R, Pecková K, Cvačka J. New MALDI matrices based on lithium salts for the analysis of hydrocarbons and wax esters. J Mass Spectrom. 2014;49:628–38.
18. Yew JY, Cody RB, Kravitz EA. Cuticular hydrocarbon analysis of an awake behaving fly using direct analysis in real-time time-of-flight mass spectrometry. Proc Natl Acad Sci U S A. 2008;105:7135–40.
19. Gross J. Direct analysis in real time—a critical review on DART-MS. Anal Bioanal Chem. 2014;406:63–80.
20. Yang ZH, Attygalle AB. Aliphatic hydrocarbon spectra by helium ionization mass spectrometry (HIMS) on a modified atmospheric-pressure source designed for electrospray ionization. J Am Soc Mass Spectrom. 2011;22:1395–402.
21. Cody RB, Dane AJ. Soft ionization of saturated hydrocarbons, alcohols and nonpolar compounds by negative-ion direct analysis in real-time mass spectrometry. J Am Soc Mass Spectrom. 2013;24:329–34.
22. Ng SH, Shankar S, Shikichi Y, Akasaka K, Mori K, Yew JY. Pheromone evolution and sexual behavior in Drosophila are shaped by male sensory exploitation of other males. Proc Natl Acad Sci U S A. 2014;111:3056–61.
23. Yew JY, Soltwisch J, Pirkl A, Dreisewerd K. Direct laser desorption ionization of endogenous and exogenous compounds from insect cuticles: practical and methodologic aspects. J Am Soc Mass Spectrom. 2011;22:1273–84.
24. Sherrod SD, Diaz AJ, Russell WK, Cremer P, Russell DH. Silver nanoparticles as selective ionization probes for analysis of olefins by mass spectrometry. Anal Chem. 2008;80:6796–9.
25. Sekuła J, Niziol J, Rode W, Ruman T. Silver nanostructures in laser desorption/ionization mass spectrometry and mass spectrometry imaging. Analyst. 2015;140:6195–209.

26. Schnapp A, Niehoff AC, Koch A, Dreisewerd K. Laser desorption/ionization mass spectrometry of lipids using etched silver substrates. Methods. 2016;104:194–203.
27. Carlson DA, Geden CJ, Bernier UR. Identification of pupal exuviae of Nasonia vitripennis and Muscidifurax raptorellus parasitoids using cuticular hydrocarbons. Biol Control. 1999;15:97–106.
28. Steiner S, Mumm R, Ruther J. Courtship pheromones in parasitic wasps: comparison of bioactive and inactive hydrocarbon profiles by multivariate statistical methods. J Chem Ecol. 2007;33:825–38.
29. Niehuis O, Büllesbach J, Judson AK, Schmitt T, Gadau J. Genetics of cuticular hydrocarbon differences between males of the parasitoid wasps *Nasonia giraulti* and *Nasonia vitripennis*. Heredity. 2011;107:61–70.
30. Giesbers MCWG, Gerritsma S, Büllesbach J, Diao W, Pannebakker BA, van de Zande L, et al. Prezygotic isolation in the parasitoid wasp genus Nasonia. Speciation: natural processes, genetics and biodiversity. Hauppauge: Nova Science Publishers; 2013.
31. Büllesbach J, Gadau J, Beukeboom LW, Echinger F, Raychoudhury R, Werren JH, et al. Cuticular hydrocarbon divergence in the jewel wasp *Nasonia*: evolutionary shifts in chemical communication channels? J Evol Biol. 2013;26:2467–78.
32. Büllesbach J, Greim C, Raychoudhury R, Schmitt T. Asymmetric assortative mating behaviour reflects incomplete pre-zygotic isolation in the *Nasonia* species complex. Ethology. 2014;120:834–43.
33. Mair MM, Kmezic V, Huber S, Pannebakker BA, Ruther J. The chemical basis of mate recognition in two parasitoid wasp species of the genus Nasonia. Entomol Exp Appl. 2017;164:1–15.
34. Steiner S, Hermann N, Ruther J. Characterization of a female-produced courtship pheromone in the parasitoid Nasonia vitripennis. J Chem Ecol. 2006;32:1687–702.
35. Büllesbach J, Vetter SG, Schmitt T. Differences in the reliance on cuticular hydrocarbons as sexual signaling and species discrimination cues in parasitoid wasps. Front Zool. 2018;15:22.
36. Ruther J, Stahl LM, Steiner S, Garbe LA, Tolasch TA. Male sex pheromone in a parasitic wasp and control of the behavioral response by the female's mating status. J Exp Biol. 2007;210:2163–9.
37. Niehuis O, Büllesbach J, Gibson JD, Pothmann D, Hanner C, Mutti NS, et al. Behavioural and genetic analyses of Nasonia shed light on the evolution of sex pheromones. Nature. 2013;494:345–8.
38. Blaul B, Steinbauer R, Merkl P, Merkl R, Tschochner H, Ruther J. Oleic acid is a precursor of linoleic acid and the male sex pheromone in Nasonia vitripennis. Insect Biochem Mol Biol. 2014;51:33–40.
39. Soltwisch J, Souady J, Berkenkamp S, Dreisewerd K. Effect of gas pressure and gas type on the fragmentation of peptide and oligosaccharide ions generated in an elevated pressure UV/IR-MALDI ion source coupled to an orthogonal time-of-flight mass spectrometer. Anal Chem. 2009;81:2921–34.
40. Pirkl A, Meier M, Popkova J, Letzel M, Schnapp A, Schiller J, et al. Analysis of free fatty acids by ultraviolet laser desorption ionization mass spectrometry using insect wings as hydrophobic sample substrate. Anal Chem. 2014;86:10763–71.
41. Kühbandner S, Ruther JJ. Solid phase micro-extraction (SPME) with in situ transesterification: An easy method for the detection of non-volatile fatty acid derivatives on the insect cuticle. J Chem Ecol 2015;41:584–592.
42. Thompson SN, Barlow JS. The fatty acid composition of parasitic hymenoptera and its possible biological significance. Ann Entomol Soc Am. 1974;67:627–32.
43. Brandstetter B, Ruther J. An insect with a delta-12 desaturase, the jewel wasp Nasonia vitripennis, benefits from nutritional supply with linoleic acid. Naturwissenschaften. 2016;103:40.
44. Ruther J, Thal K, Steiner S. Pheromone communication in Nasonia vitripennis: abdominal sex attractant mediates site fidelity of releasing males. J Chem Ecol. 2011;37:161–5.
45. Drijfhout F, Kather R, Martin S. The role of cuticular hydrocarbons in insects. In: Zhang W, Liu H, editors. Behavioral and chemical ecologoly. Hauppauge: Nova Science Publishers; 2010. p. 91–114.
46. Jansen J, Pokorny T, Schmitt T. Disentangling the effect of insemination and ovary development on the cuticular hydrocarbon profile in the bumblebee Bombus terrestis (Hymenoptera: Apidae). Apidologie. 2016;47:101–13.